4th Specialty Conference on Coastal, Estuary and Offshore Engineering
4e Conférence spécialisée sur l'ingénierie côtière et en milieu maritime

Montréal, Québec
May 29 to June 1, 2013 / *29 mai au 1 juin 2013*

Effects of Tidal Power Generation on Hydrodynamics and Sediment Processes in the Upper Bay of Fundy

R.P. Mulligan[1], P.C. Smith[2], P.S. Hill[3], J. Tao[3], D. van Proosdij[4]
[1]Department of Civil Engineering, Queen's University
[2]Bedford Institute of Oceanography
[3]Department of Oceanography, Dalhousie University
[4]Department of Geography, Saint Mary's University

Abstract: The upper Bay of Fundy in Nova Scotia is known for its large tidal range, high current velocities and extensive intertidal flats with fine sediments. This region is actively being studied as a candidate for in-stream tidal power generation using an array of large turbines on the seabed. We present observations of current velocities in Minas Passage and Minas Basin that, in combination with total suspended matter estimates from the satellite-based MERIS sensor, were used to characterize the system and calibrate a hydrodynamic and sediment transport model. This has elucidated strong trends in surficial suspended sediment concentrations in the central part of Minas Basin on the seasonal timescale, ranging from less than 10 g/m^3 in the summer to 10-30 g/m^3 in the winter. Model results suggest that lower sediment concentrations in the water column may occur because critical bed shear stress values are higher, due to biological activity in the sediments in summer. This result emphasizes the sensitivity of the system to flow and sediment properties that undergo seasonal changes. Using increased flow drag to simulate in-stream turbines in Minas Passage, the model was applied to turbine array scenarios to determine possible far-field effects of tidal energy dissipation in Minas Passage on sediment processes throughout Minas Basin.

1. Introduction

Minas Basin is a semi-diurnal macrotidal embayment located at the eastern end of the Bay of Fundy in Nova Scotia (Fig. 1), and is known for its nearly resonant tides that produce a tidal range of up to 16 m (Garrett, 1972). The basin is connected to the greater Bay of Fundy via Minas Channel (15 km wide) and Minas Passage, which narrows to a width of approximately 4.5 km. In Minas Channel tidal current speeds can reach 4-5 m/s, making this region a site of interest for in-stream tidal power generation. The seabed varies greatly in sediment texture and water depth from exposed bedrock in a 170 m scour trench in Minas Passage (Parrott, 2008) to sand and gravel deposits in the central part of the basin with a mean depth of 15 m at low tide (Amos and Long, 1980) to shallow intertidal estuarine mudflats along the edge of the basin (Amos et al., 1988). The surface waters in intertidal areas have very high suspended sediment concentrations that can exceed 200 g/m^3, and are carried by tidal currents into the basin.

The development of numerical models to understand the physics of tides in the Bay of Fundy was pioneered by Greenberg (1979). Greenberg and Amos (1983) examined the transport of suspended sediments using a numerical model, and considered the effects of constructing a tidal barrage for energy extraction. Recently, considerable research effort has gone into developing numerical models for predicting impacts of tidal energy extraction. Karsten et al. (2008) examined the maximum power production over a tidal cycle from in-stream turbines placed in Minas Passage by using the finite-volume
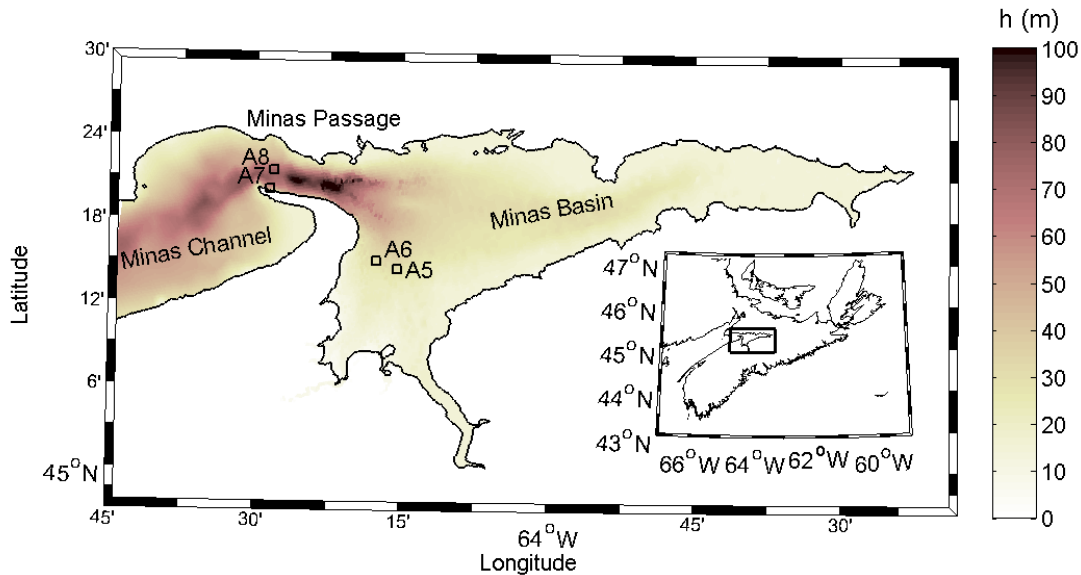
Figure 1: Location map of Nova Scotia (inset) and bathymetry of Minas Channel and Minas Basin for the Delft3D model domain. ADCP instrument locations in July-August 2009 are indicated (A5-A8).

coastal ocean model (FVCOM). The effect of turbine drag (parameterized by an increased bottom drag coefficient) on the flow through the Minas Passage was used to predict the resulting tidal amplitudes in Minas Basin for various turbine scenarios. Hasegawa et al. (2011) determined tidal circulation using a nested-grid version of the Princeton Ocean Model (POM). They studied energy extraction using quadratic friction in the momentum equation to determine far-field effects on tidal amplitudes in the Bay of Fundy and the Gulf of Maine. Wu et al. (2011) used FVCOM to simulate tidal flows and examined the transport of bedload and suspended sediments in Minas Basin.

In this study we examine the changes in flow and suspended sediments that could result as the system adjusts to a new equilibrium after deployment of an array of tidal turbines across Minas Passage. The case of a major turbine array to extract the maximum available power is investigated, as determined by the results of Karsten et al. (2008) and Hasegawa at al. (2011). To accomplish this, we use the Delft3D numerical hydrodynamic and sediment transport model (Lesser et al., 2004) and represent the turbines as a semi-permeable thin hydraulic structure with quadratic friction term prescribed over the lower half of the water column. Observations of tidal currents from bottom-mounted Acoustic Doppler Current Profilers (ADCPs) and satellite-derived near-surface suspended sediment concentrations are presented in Section 2, and used to validate the predicted hydrodynamics and sediment dynamics for a period in July-August, 2009 (Section 3). Discussion and conclusions are presented in Section 4, where changes to suspended sediment concentrations in tidal estuaries induced by tidal energy extraction devices are assessed.

2. Observations

2.1 ADCP Data

A subset of the multi-year current meter data collected in Minas Basin is used in this study, for the period of July 17 to August 14, 2009. Current profiles were collected by the Bedford Institute of Oceanography at four locations shown in Fig. 1. Two instruments were located in Minas Passage (A7, A8) and two instruments were located in Minas Basin (A5, A6). The sensors were RDI ADCPs that were deployed in a bottom-mounted upward-looking mode and operated at 300 kHz to collect hourly-averaged current data in 2 m vertical bins. At the same time acoustic sensors, optical backscatter sensors and sediment traps were deployed in an intertidal creek in the Cornwallis River Estuary, in the southern part of Minas Basin.

The velocity data indicate strong tidal currents that are modulated over daily and spring-neap tidal cycles. In Minas Passage, speeds can be up to 5 m/s (at A8) and recirculation can occur along the southern shore near Cape Split (at A7). In Minas Basin the flows can reach 1.5 m/s (at A5, A6) and are as low as 0.01-0.05 m/s in intertidal areas. Observations of suspended sediment concentration (SSC) using optical backscatter sensors deployed in terminal creeks in the Cornwallis River Estuary, indicate very high SSC of up to 200-400 g/m^3 with significant variability over tidal and seasonal cycles.

2.2 MERIS Satellite Data

Remote sensing of ocean colour from space has allowed sediment properties over large spatial scales to be observed. In several cloud free days in August 2009, the MEdium Resolution Imaging Spectrometer (MERIS) observed the surface layer of the Bay of Fundy. MERIS was a scientific instrument on board the European Space Agency (ESA) Envisat Earth-orbiting satellite that operated from 2002-2012. From the near daily synoptic MERIS data at 300 m resolution, the total suspended matter (TSM) concentration is derived from empirical relationships and is equivalent to the suspended sediment concentration (SSC) referred to hereafter. This has elucidated strong trends in SSC over seasonal timescales, with concentrations ranging from 10-30 g/m^3 in the winter to less than 10 g/m^3 in the summer in the central part of Minas Basin (Tao, 2013). As an example, this difference is shown by the instantaneous observations of SSC in winter and summer in Fig. 2 where the dominant spatial trend is typically a westward and northward reduction in concentration from intertidal to deeper areas. Biofilms are being investigated as a cause for seasonal changes in SSC. Sediment biofilms associated with diatoms and cyanobacteria increase cohesiveness of sediments, which reduces erosion rates and SSC in summer. In winter, reduction or removal of biofilms would result in less cohesion between particles, increasing sediment erosion rates.
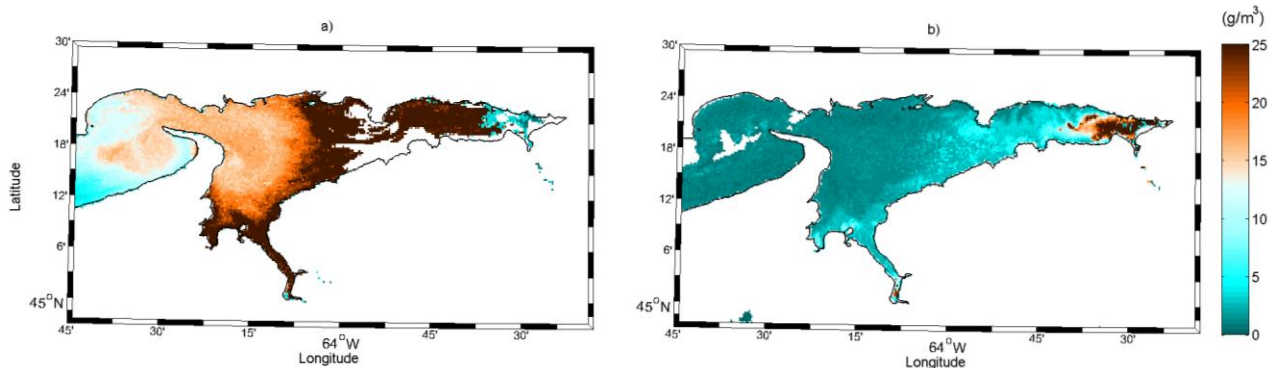

Figure 2: Representative instantaneous observations of suspended sediment concentration (g/m^3) at the water surface determined from MERIS ocean colour imagery in: a) winter (15:00 Feb. 25, 2009); and b) summer (15:00 Aug. 17, 2009). White areas indicate places where the sea surface was obscured by cloud cover.

3. Model

3.1 Model Description

In this study we examine sediment transport using a hydrodynamic and morphologic model, Delft3D (Lesser et al., 2004). Delft3D is a finite-difference model that numerically solves the horizontal momentum equations. The sediment component includes parameterizations of hydrodynamic roughness in the bottom boundary layer, bedload and suspended-load transport, and deposition, erosion, and evolution of bed morphology. Elias et al. (2006) used Delft3D to predict sand transport and morphological response for strong tidal flows through inlets in the Netherlands barrier island chain. Mulligan et al. (2008) used the

hydrodynamic model to determine the relative magnitudes of currents driven by different forcing mechanisms including tides, storm surges, surface waves and winds in Lunenburg Bay, NS. Cohesive sediments and bed stability induced by biological activity in the Wadden Sea has been examined using Delft3D by Borsje et al. (2008).

The bathymetric grid for Minas Basin was constructed by combining existing hydrographic survey charts with high-resolution multi-beam bathymetry (Parrott et al., 2008) over some of the area. The data were interpolated onto a spherical structured grid (Fig. 1) that extended 105 km in the east-west (x) direction and 45 km in the north-south (y) direction with horizontal resolution of 170 m in the x-direction by 200 m in the y-direction. The vertical grid has 10-layers in topography-following σ-coordinates, and the model was run in three-dimensional mode using a time step of 30 s with the open boundary placed at the western end of Minas Channel. Following an initial spin-up time, the model was run for the period of ADCP observations (Jul. 17 – Aug. 14, 2009) using a water-level boundary condition developed from tidal prediction using WebTide (Dupont et al., 2002) with the 5 primary tidal constituents (M_2, N_2, S_2, K_1, O_1) shown in Fig. 3. The bottom friction coefficient was set to the canonical value of $C_D = 0.0023$.
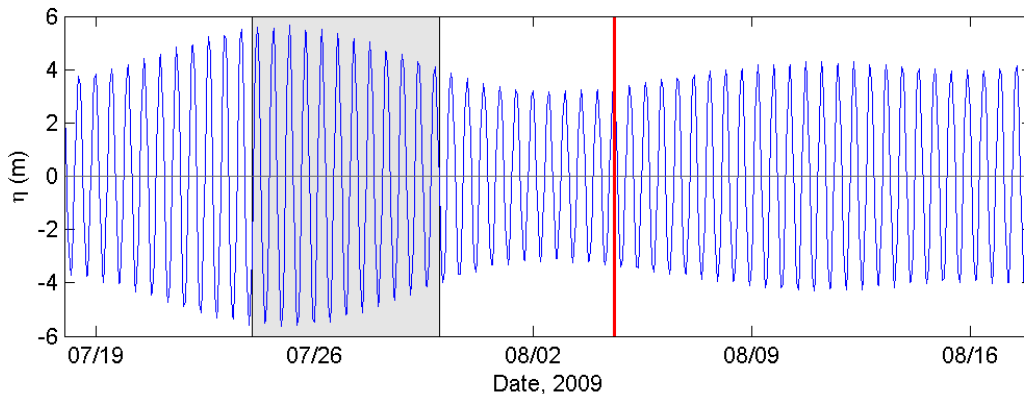

Figure 3: Time series of tidal elevations (η) above the mean water level used as model forcing at the open boundary. The shaded box indicated the spring tides shown in Fig 5. and the red line indicates the time of the MERIS image in Fig 7.

SSC was initialized at zero, therefore requiring modelled suspended sediments to be eroded from the bed. The initial conditions on the bed were developed from bottom texture observations of Amos and Long (1980) where most sediments in the central part of Minas Basin are non-cohesive (sands to gravels) with relatively high settling velocities and fine cohesive sediments (muds) in several locations around the rim of the basin (namely the Cornwallis River estuary, the Avon River channel, near Economy Point, and Cobequid Bay). A simple bi-modal distribution map that resembles the Amos and Long (1980) observations was developed to describe the initial seabed conditions, consisting of fine mud in water depths of 10 m and less (relative to the mean sea level datum) and sand in depths greater than 10 m. A series of sensitivity tests for varying sediment properties (e.g. grain size, settling velocity, critical shear stress) was completed to determine the summer and winter sediment conditions, after comparison with satellite imagery (Tao, 2013). For the sand layer, a mean grain diameter (d_{50}) of 2 mm was used with the non-cohesive sediment formulation (Van Rijn, 2007). Model results indicate that these particles are transported as bedload and suspended load during ebb and flood phases of the tide, with highest concentrations in Minas Channel where currents are strongest. However the coarse particles have a high settling velocity and sink out of suspension with slackening of the tidal currents. For the cohesive intertidal mud layer, a settling velocity of 0.1 mm/s was used, corresponding to a grain size of less than 100 μm, and the critical shear stress for erosion (τ_{cr}) was varied based on values determined by Amos et al. (1992) for bed sediment samples on the tidal flat of the Cornwallis river estuary. Across the 2.5 km wide mudflat they measured a range of in situ bed shear stresses: 0.1-7.5 N/m^2 (during July and August, 1989-1990). In this case, we used a high critical bed shear stress of erosion $\tau_{cr} = 4$ N/m^2 to represent high particle cohesion in summer months.

3.2   Representation of In-Stream Turbines

To simulate the effects of turbines in model grids where individual turbine structures cannot be resolved, Karsten et al. (2008) locally modified bottom friction in Minas Passage and Hasegawa et al. (2011) introduced a quadratic friction term in the water column. In this study, we simulate the turbines by introducing a semi-permeable barrier to the flow over part of the water depth with momentum losses parameterized by quadratic friction. The bulk effects of an array of turbines were investigated by implementing a "porous plate" across Minas Passage. This is a thin hydraulic structure relative to the model grid size that acts as a semi-permeable barrier to the flow over only part of the water column and adds friction to the flow. The porous plate is a partially transparent structure that extends into the flow for all or some vertical layers, across which some mass and momentum can be exchanged. The porosity is controlled by an energy loss coefficient that is prescribed across the height of the structure. This adds drag in the horizontal momentum equations (e.g., Lesser et al., 2004). The momentum equation for flow in the x-direction can be simplified as:

[1] $\partial u/\partial t + M_A - fv = - M_P + M_M - M_B - M_T$

where u and v are velocity components in the x- and y-directions respectively, t is time, M_A represents the advective terms, f is the Coriolis parameter, M_P is the pressure gradient, M_M represents mixing terms and M_B is the bottom friction. The momentum sink for the combined effect of turbines is given by:

[2] $M_T = c_L/\Delta y \ u \ (u^2+v^2)^{1/2}$

where c_L is a dimensionless loss coefficient and Δy is the grid resolution in the y-direction. In this case, we have implemented a turbine array that extends vertically over half of the water column from the bottom to mid-depth (σ = 5-10) and is oriented in the y-direction so as to impede flow in the x-direction with c_L = 100, such that $c_L/\Delta y$ = 0.5. This caused a reduction of momentum at the turbine array in the lower half of the flow only and surface currents can flow over the submerged turbines as indicated in Fig. 4. The reduction in local momentum decreases the flow velocity around the structure, which influences a large region in Minas Basin. As a result the bottom friction, which is also a function of flow velocity, is reduced in magnitude over the affected area.
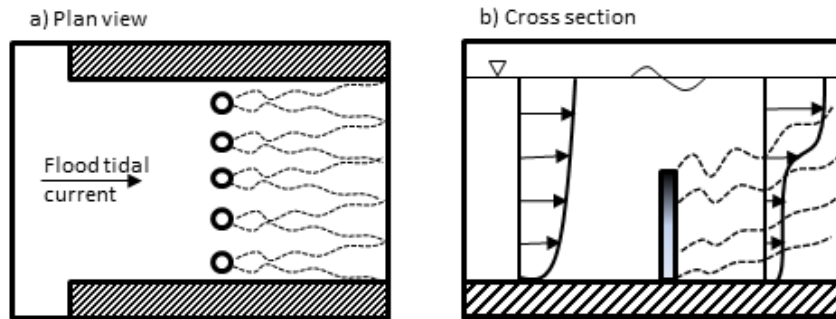

Figure 4: Schematization of turbine implementation, a) plan view of an idealized turbine array across Minas Passage and flow drag added by the structures; b) cross-section showing modification of the velocity profile due to drag added by the bottom-founded porous plate.

4   Results

4.1   Hydrodynamics

The observed near-surface currents in Minas Passage (A8) and in Minas Basin (A5) are shown in Fig. 5a,d for a subset of the data for the highest monthly (spring) tides. The mean water depths at these sites are 67 m (at A8) and 20 m (at A5), and the near-surface acoustic bin location varies in depth from 2 m below the water surface at low tide to 18 m below the water surface at high tide. In the model the surface layer thickness, which varies with water depth, is 6.1 to 7.3 m thick (at A8) and 1.4 m to 2.6 m thick (at A5). The semi-diurnal signal has magnitudes at A8 up to 5.2 m/s over this time, with most of the flow in the east-west direction (u component) and flood currents that are stronger than ebb. At A5 the currents are up to 1.4 m/s with a stronger north-south (v) component. The predicted currents agree well with the magnitude and phase of the observations at both sites (Fig. 5b,e), although the model over-predicts the currents in Minas Passage by up to 9% for the spring tides. For the no extraction case, the maximum current magnitudes during spring tides were 5.7 m/s at A8 and 1.4 m/s at A5 in the surface layer over the period. When the turbines are added to Minas Passage, the additional drag on the flow resulted in predicted currents that reduced to 4.4 m/s and 0.9 m/s (Fig. 5c,f).
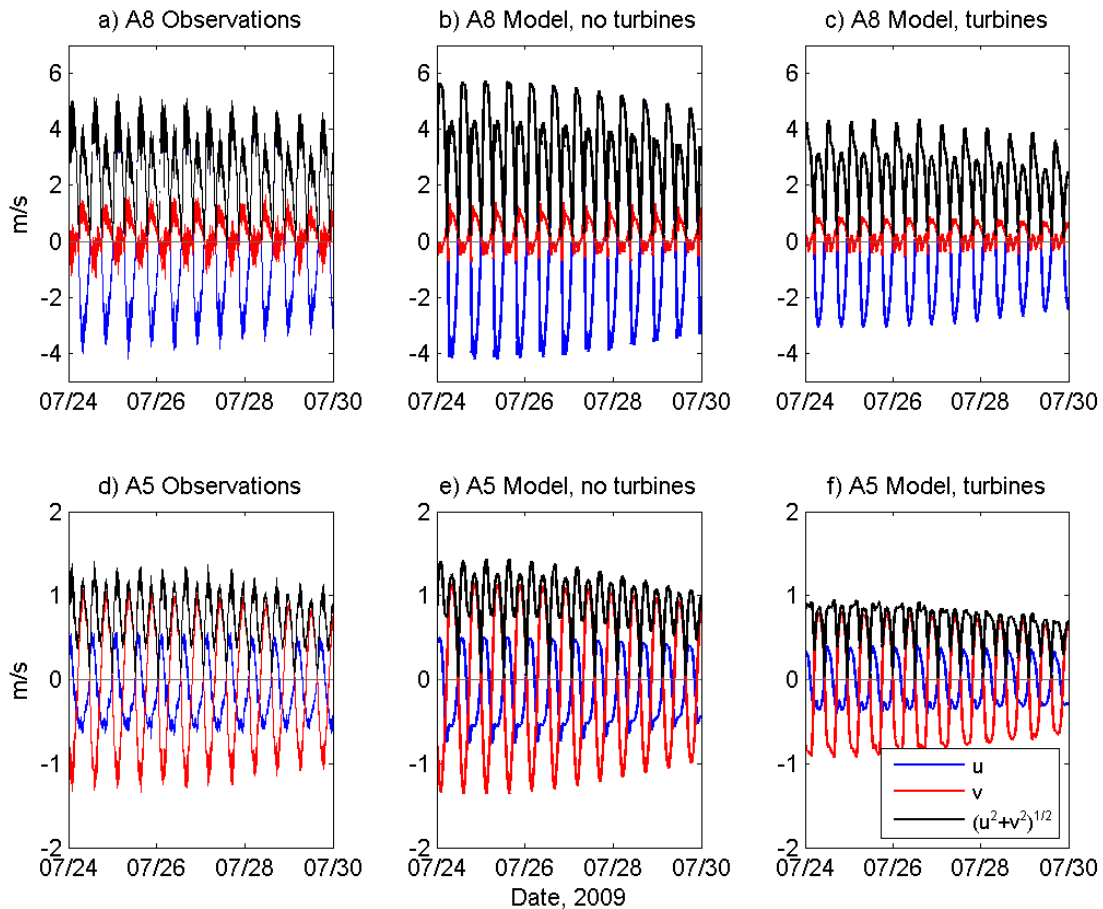

Figure 5: Time series of near-surface tidal current velocity components (u,v) and speed (s) at sites A8 and A5 from ADCP observations and model results without and with turbines implemented in Minas Passage. Correlations coefficients for u,v are 0.98,0.81 at A8 and 0.98,0.94 at A5 over the 1 month simulation.

The spatial variability of the depth-averaged flow in Minas Passage on a flood tide is shown in Fig. 6 for the case of no extraction and for turbine implementation. Although the turbines are only in the lower half of the water column, the added drag has a strong influence on the flow throughout Minas Passage. Consequently this results in lower flows throughout Minas Basin, lower bed shear stresses and less re-suspension of fine sediments in coastal areas. The changes in velocity are strongest in Minas Passage, and are significant throughout Minas Basin to the east and toward the model boundary in Minas Channel to the west. This represents the extreme case for maximum tidal power extraction, and other cases representing different turbine arrays will be investigated in other studies.
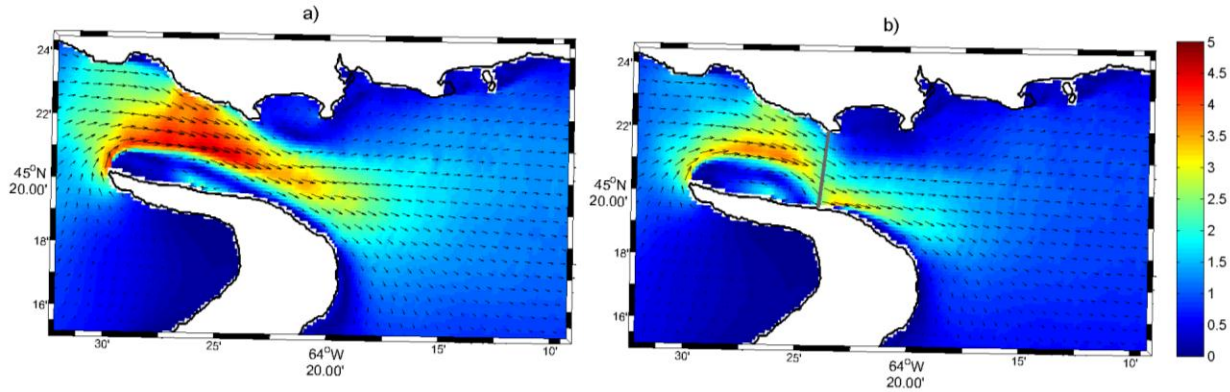

Figure 6: Model predictions of depth-averaged tidal current velocities (m/s) during flood tide on Aug. 4, 2009: a) no extraction case, b) turbines implemented and denoted by the line across Minas Passage.

4.2   Suspended Sediments

The predicted SSC is shown in Fig. 7b for a time corresponding to ebb tidal flow just after high tide (Fig. 3) that was observed by MERIS (Fig. 7a). The results for the no-extraction case suggest that the model adequately simulates some important sediment transport phenomena, including higher surface SSC in the source areas (tidal flats and river mouths in Cobequid Bay and the Southern Bight of Minas Basin), lower SSC in the central part of Minas Basin and in Minas Passage. The model also suggests strong variability in SSC over a tidal cycle. At A5 the model predicted SSC to be in the range 0.1-0.5 g/m^3 over the tidal cycle, where sediments have advected from shallow intertidal areas to the central part of the basin. In comparison, the satellite observed surface SSC at A5 were also low (<1 g/m^3). The model used a high τ_{cr} in this simulation to represent summer sediment conditions with high cohesion due to biological activity. To represent winter sediment conditions (lower cohesion due to less biological activity) τ_{cr} was decreased to 1 N/m^2, resulting in higher surface SSC of 1-50 g/m^3 at A5 over a tidal cycle with similar tidal forcing. Values observed by satellite were also higher (10-30 g/m^3) in winter 2009. These results indicate that the system is very sensitive to τ_c and other sediment input properties, and seasonal changes in sediment properties that increase the cohesion may explain the order-of-magnitude change in sediment volume in suspension.

For the case with turbines implemented in Minas Passage and c_L = 100, the surface SSC in Minas Basin (Fig. 7c) is significantly lower than when no extraction occurs (Fig. 7b). In order to compare the two cases, we define Minas Basin as the area east of 64.3°W longitude. In this region, the root-mean-square (RMS) velocity is 1.4 m/s (no turbines) and 1.0 m/s (turbines), and the mean SSC is 4.9 g/m^3 (no turbines) and 1.4 g/m^3 (turbines). This represents reductions of velocity by 28% and SSC by 71% by introducing turbines. Reducing the loss coefficient to c_L = 10 for the turbines results in an RMS velocity of 1.1 m/s and mean SSC of 2.6 g/m^3, representing reductions of velocity by 21% and SSC by 47% for a smaller turbine array.
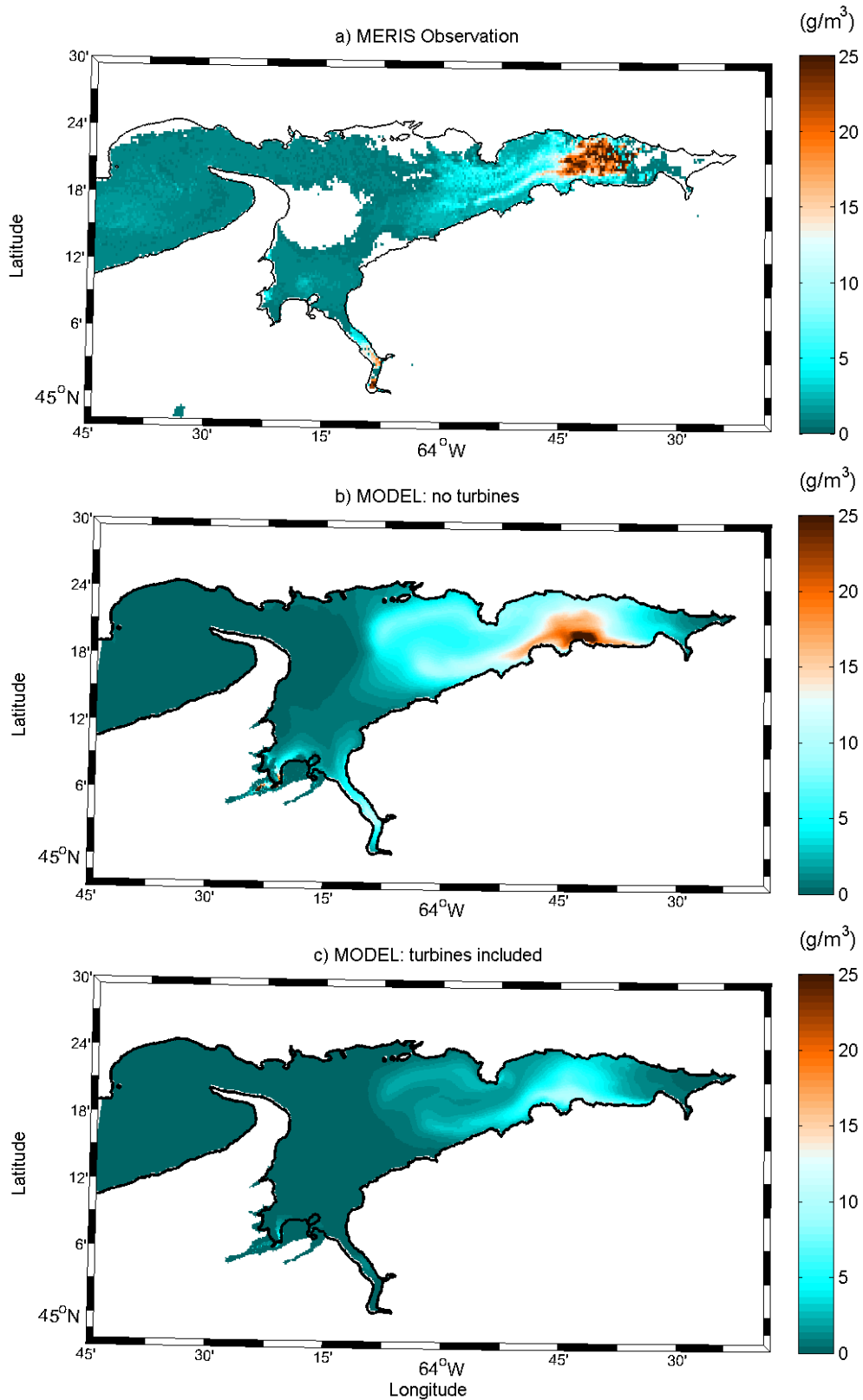
Figure 7: Surface suspended sediment concentration on an ebb tide in Minas Basin at 14:00 Aug. 4, 2009: a) MERIS observations (white areas indicate places where the sea surface was obscured by cloud cover); b) model with no turbines; c) model with turbines across Minas Passage.

5 Discussion and Conclusions

Sensitivity tests for lower values of c_L to represent smaller or fewer turbines indicate that the reduction in RMS velocities and SSC in Minas Basin are not as high but the trend is the same: the turbines in Minas Passage that extract energy reduce potential and kinetic energy in Minas Basin. This reduces bottom shear stresses and suspended sediment concentrations, and leads to higher sedimentation rates and siltation in channels. The magnitude of these changes will be determined by the number and size of turbines, which should be determined by optimizing the power output. Karsten et al. (2008) found that extraction of the maximum power of 6.95 GW from turbines in Minas Passage could result in a 36% reduction of M_2 tidal amplitudes in Minas Basin. The results of Hasegawa et al. (2011) indicate a 41% reduction in tidal amplitudes for the highest 3 tidal constituents (M_2, N_2, S_2) in Minas Basin for their higher estimate of maximum turbine power of 7.6 GW. Although the parameterizations of the turbines are different for these studies, we find a 23% reduction in tidal amplitude at site A5 in Minas Basin for the turbine scenario presented here (which corresponds to approximately 6.0 GW of power extracted after comparison with the results of Karsten (2008)). Reducing the value of c_L by an order of magnitude from 100 to 10 results in a 14% reduction of tidal amplitude at A5 (which corresponds to approximately 5.0 GW of power extracted) when compared to the no extraction case.

The present results are in reasonable agreement with the hydrodynamic results of other studies and are useful for understanding changes to suspended sediments in Minas Basin under near-maximum turbine power extraction conditions. For highly cohesive "summer"-type sediment properties, parameterized by a high critical shear stress of erosion, it is anticipated that suspended sediment concentrations in Minas Basin could be reduced by up to 71% after introducing turbines in Minas Passage, leading to higher sediment deposition rates on tidal flats and in channels.

Acknowledgments

References

Amos, C.L., and Long, B.F.N.1980. The sedimentary character of the Minas Basin, Bay of Fundy. In The Coastline of Canada, S.B., McCann (ed.), Geological Survey of Canada, Paper 80-10, pp. 123-152.

Amos, C.L., Van Wagoner, N.A. and Daborn, G.R. 1988. The influence of subaerial exposure on the bulk properties of fine-grained intertidal sediment from Minas Basin, Bay of Fundy. *Estuarine, Coastal snd Shelf Sci.*, 27: 1-13.

Amos, C.L., Daborn, G.R., Christian, H.A., Atkinson, A., and Robertson, A. 1992. In situ erosion measurements on fine-grained sediments from the Bay of Fundy, *Marine Geology*, 108(2), 175-196.

Borsje, B.W., de Vries, M.B., Hulscher, S., and de Boer, G.J. 2008. Modeling large-scale cohesive sediment transport affected by small-scale biological activity. *Estuarine, Coastal and Shelf Sci.,* 78: 468-480.

Dupont, F., Hannah, C., Greenberg, D.A., Cherniawsky J., and Naimie, C., 2002. Modelling system for tides, *Can. Tech. Rep. Hydrogr. Ocean Sci.,* 221, 72 pp.

Elias, E.P.L., Cleveringa, J., Buijsman, M.C., Roelvink, J.A., and Stive, M.J.F. 2006. Field and model data analysis of sand transport patterns in Texel Tidal inlet (the Netherlands), *Coastal Eng.*, 53:505-529.

Garrett, C. 1972**.** Tidal resonance in the Bay of Fundy and Gulf of Maine, *Nature*, 238: 441–443.

Greenberg, D.A. 1979. A numerical model investigation of tidal phenomena in the Bay of Fundy and Gulf of Maine, *Marine Geodesy*, 2(2): 161-187.

Greenberg, D.A., and Amos, C.L. 1983. Suspended Sediment Transport and Deposition Modeling in the Bay of Fundy, Nova Scotia - a Region of Potential Tidal Power Development, *Can. J. of Fisheries and Aquatic Sci.,* 40 (suppl. 1), 20-34.

Hasegawa, D., Sheng, J., Greenberg, D.A., and Thompson, K.R. 2011. Far-field effects of tidal energy extraction in the Minas Passage on tidal circulation in the Bay of Fundy and Gulf of Maine using a nested-grid coastal circulation model, *Ocean Dynamics*, 61(11):1845-1868.

Karsten, R.H., McMillian, J.M., Lickley, M.J. 2008. Assessment of tidal current energy in Minas Passage, Bay of Fundy. Proc. IMechE, Part A: J Power Energy, 222:493–507.

Lesser, G., Roelvink, J., van Kester, J., and Stelling, G. 2004. Development and validation of a three-dimensional morphological model, *Coastal Eng.*, 51: 883-915.

Mulligan, R.P., Hay, A.E., and Bowen, A.J. 2008. Wave-driven circulation in a coastal bay during the landfall of a hurricane, *Journal of Geophysical Research Oceans*, 113, C05026.

Parrott, D.R., Todd, B.J., Shaw, J., Clarke, J.E.H., Griffin, J., MacGowan, B., Lamplugh, M., and Webster, T. 2008. Integration of multibeam bathymetry and LiDAR surveys of the Bay of Fundy, Canada., *Proc. the Canadian Hydrographic Conf. and National Surveyors Conf.*, Victoria, BC.

Tao, J. 2013. Temporal autocorrelation analysis to identify the dominant time scales of suspended sediment variability in Minas Basin, MSc Thesis, Dalhousie University, *in draft.*

Van Rijn, L.C. 2007. Unified view of sediment transport by currents and waves II: Suspended transport, *J. of Hydraulic Eng.*, 133(6): 668-689.

Wu, Y., Chaffey, J., Greenberg, D.A., Colbo, K., and Smith, P.C. 2011. Tidally-induced sediment transport patterns in the upper Bay of Fundy: a numerical study, *Continental Shelf Research,* 31: 2041–2053.